

Vertical Axis Wind Turbine development

Guilherme Silva

Abstract: Wind power is, nowadays, the most promising and suitable renewable energy for rapid and cost-effective implementation. Horizontal axis wind turbines have been greatly developed but some other technologies, such as the vertical axis wind turbines are still in an initial development phase. The disparity in the development of these technologies remains unexplained. Nevertheless, the little development made in vertical axis wind turbines seems to emphasize this technology as being one of great potential. This present work aimed to create an analysis of this technology. Models were developed, and a wide range of CFD results were obtained using the kw SST model. In the end, a small wind turbine intentionally built for this work was tested.

Keywords: VAWT Darrieus Giromill H-rotor Vertical axis wind turbine Wind power Kw model.

V_i	Induced velocity;
V_p	Blade's flow velocity;
V_{rated}	Nominal velocity;
V_∞	Wind velocity;
α	Angle of attack;
θ	Angular position;
λ	Tip speed ratio;
ρ	Density;
σ	Solidity;
ω	Angular velocity;
ν	Kinematic viscosity.

ABBREVIATIONS AND ACRONYMS

A	Area;
AR	Aspect ratio;
c	Blade chord;
C_D	Drag coefficient;
C_L	Lift coefficient;
C_p	Power coefficient;
COE	Cost of energy;
D	Drag;
EU	European Union;
f	Frequency;
F	Force;
F_n	Lateral force;
F_t	Tangential force;
$HAWT$	Horizontal axis wind turbine;
I	Moment of inertia;
L	Lift;
LC	Lifetime costs;
LEO	Lifetime energy output;
M	Torque;
n	Number of blades;
P	Power;
r	Radius;
Re	Reynolds number;
t	Time;
V	Velocity;
$VAWT$	Vertical axis wind turbine;
V_{cut_in}	Start-up velocity;
V_{cut_out}	Maximum velocity;

I. INTRODUCTION

Wind energy is the energy from the wind. This form of energy can be converted to other more useful forms such as electricity, through the use of wind turbines.

Wind power is the power, in W, given by the kinetic energy of wind in a given area, per unit of time^[3]:

$$P_{wind} = \frac{1}{2} \rho A V_\infty^3, \quad (1)$$

being ρ is the density of air in kg/m³, A the area considered in m² and V_∞ the wind velocity in m/s.

Worldwide, the use of wind power has been rising, around 25% per year, since the early 1990s. This increase has been stronger in Europe. In the future, this trend is expected to continue mainly through the use of offshore areas^[5].

The efficiency of wind turbines is normally characterized by the power coefficient^[3]:

$$C_p = \frac{P_{turbine}}{P_{wind}} = \frac{P_{turbine}}{\frac{1}{2} \rho A V_\infty^3}. \quad (2)$$

Wind turbines can be divided into two types. In drag turbines, movement is produced by the air drag while in lift turbines movement is produced by the air lift in the turbine's blades. One of the most important concepts of wind turbines is the tip speed ratio defined as

$$\lambda = \frac{\omega r}{V_\infty}, \quad (3)$$

being ωr the blade's velocity in m/s and V_∞ the wind velocity in m/s^[1].

In drag turbines, theoretically, $\lambda < 1$. Drag turbines also tend to start movement at lower V_∞ but have high drag at high V_∞ . On the other hand, lift turbines have starting problems, usually needing help to start but have lower drag at high V_∞ and usually superior C_p ^[1].

Wind turbines can also be divided into HAWT (Horizontal Axis Wind Turbine) and VAWT (Vertical Axis Wind Turbine). VAWTs seem to have easier maintenance, less noise and do not need alignment with the wind^[1,3].

Many types of wind turbines have been developed as shown in Figure 1.

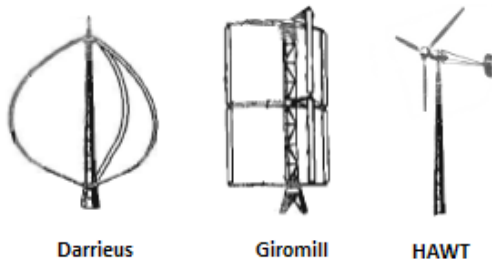


Figure 1 – Types of wind turbines

The most widely spread type of wind turbine is the 3-bladed HAWT, but other types have demonstrated good feasibility, such as the Darrieus or the giromill turbine. The giromill turbine, using untwisted straight blades allows an easier construction and transport, reducing costs^[1].

The Betz's limit is the theoretical maximum C_p value:

$$C_{p \max} = \frac{16}{27} \approx 59\% \quad (4)$$

calculated assuming an ideal turbine, with infinite number of blades, without losses^[3].

II. WORKING PARAMETERS

Although giromill VAWTs are the simplest type of wind turbine, its aerodynamic analysis is very complex^[1]. Consider a turbine with radius r , spinning at ω angular velocity within a flow with velocity V_∞ . The blade's wind velocity V_p can be decomposed into its normal component V_n (pointing from inside to outside the turbine) and its tangential component V_t (pointing from the leading edge to the trailing edge):

$$V_t = r\omega + V_\infty \cos(\theta), \quad (5)$$

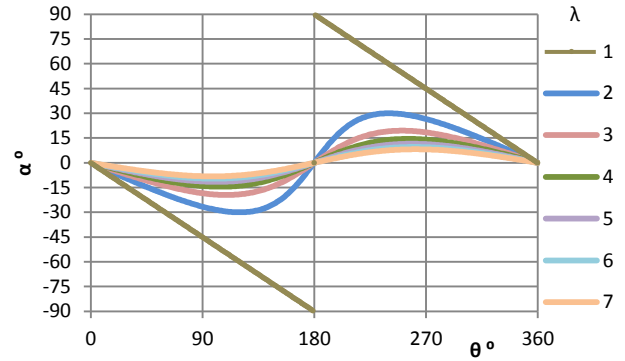
$$V_n = -V_\infty \sin(\theta). \quad (6)$$

With the increase of λ , V_t becomes the dominant component in V_p , diminishing the blade's angle of attack α ^[8]:

$$\alpha = \tan^{-1} \left(\frac{V_n}{V_t} \right). \quad (7)$$

Replacing in the previous formulas,

$$\alpha = \tan^{-1} \left(-\frac{\sin(\theta)}{\cos(\theta) + \lambda} \right). \quad (8)$$



Graph 1 – α according to θ and λ

α is independent of V_∞ and it varies less with λ increase. For $\lambda > 3$, $\alpha_{\max} < 20^\circ$.

V_p is given by^[8]:

$$V_p = \sqrt{V_t^2 + V_n^2}. \quad (9)$$

Combining the previous formulas:

$$V_p = V_\infty \sqrt{\lambda^2 + 2\lambda \cos \theta + 1}, \quad (10)$$

$$\overline{V_p} = V_\infty \sqrt{\lambda^2 + 1}, \quad (11)$$

The mean Reynolds number can be obtained by

$$\overline{Re} = \frac{V_\infty \sqrt{\lambda^2 + 1}}{\nu} c. \quad (12)$$

being c the blade's chord in m and ν the kinematic viscosity of air in m^2/s . For a VAWT with $c = 10$ cm, with $\lambda = 8$ and $V_\infty = 11$ m/s, $\overline{Re} \approx 6 \times 10^5$.

The resulting aerodynamic forces in the blades can be obtained by the interpolation of C_L and C_D according to the airfoil used and the given conditions of α and \overline{Re} . This kind of information is hard to find for typical working conditions of a VAWT (low \overline{Re} and high α)^[2].

The blade's force components can be obtained by^[8]:

$$F_t = L \sin(\alpha) + D \cos(\alpha), \quad (13)$$

$$F_n = L \cos(\alpha) + D \sin(\alpha), \quad (14)$$

as depicted in Figure 2.

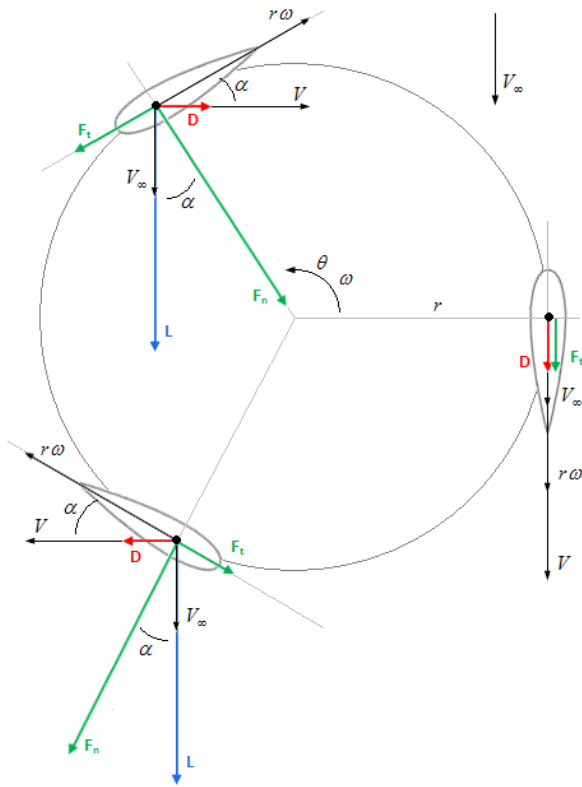


Figure 2 – VAWT's aerodynamic forces

It can be concluded that α has a primary importance in the intensity of F_t . As seen before, α depends on λ . This relationship defines the working conditions of the turbine. At low λ , α is high, making the blade stall, diminishing the L/D ratio. At high λ , α is low and the tangential component of L is small. There is an optimum λ where α is high enough for the tangential component of L to be considerable and low enough for the L/D ratio to be high. For a VAWT, optimum λ is usually between 3 and 5^[1].

According to these conclusions, an airfoil suitable for a giromill VAWT should stall at high α , allowing its use at high α (low λ), maximizing the tangential component of L , increasing F_t . On the other hand, the L/D ratio should be kept high to reduce the drag on each blade. A possible solution for both these restrictions would be the use of an airfoil with a drag bucket.

The power produced is obtained by^[8]:

$$P = M\omega, \quad (15)$$

$$M = n\overline{F_t}r. \quad (16)$$

In the turbine's blades, the quick change of α and V_p makes the blade's response dynamic, different from the results normally published in static regimes. That difference is important and depends on many factors. In these conditions, stall is denominated dynamic stall. In VAWTs, dynamic stall has been found to provide higher efficiency but also higher noise and fatigue^[2].

Parashivoiu^[1] concluded that there is no advantage in a bigger diameter, as the turbine's cost increases with the cube of the diameter while the energy captured increases with the square of the diameter (for $AR = 1$).

The increase of AR , increases ω and diminishes M (for the same amount of $P_{turbine}$). These parameters should be set according to the type of generator used. As generators tend to work at high ω , high AR turbines (high ω) are suitable for a direct connection to the generator while low AR turbines (with low ω but high M) should use a gearbox. High AR increases the amount of material and the area of the blades (a costly component). Equilibrium must be found between cost and efficiency^[1].

End/tip losses occur due to the flow from the highest pressure to the lowest pressure side of the blade's tip. This effect is attenuated by the use of high AR or wingtips. This is the main factor indicated as responsible for the differences between 2D and 3D simulations of a VAWT's flow^[10].

Solidity is a crucial parameter in VAWT development and is obtained by:

$$\sigma = nc/r \quad (17)$$

Results indicate that lower σ results in higher efficiency and optimum λ ^[1].

For a given σ is structurally more advantageous to have fewer blades with higher c ^[1]. But 3-bladed turbines have a more stable operation than 2-bladed turbines. This happens because the resulting aerodynamic forces at the blades reach maximum at each half turn. With two blades, these maximums are reached in phase^[2].

With the adequate roughness, it is possible to force the transition of a laminar boundary layer to turbulent. In VAWT, blade's roughness is an important parameter^[10].

The airfoils usually studied have been developed for the aircraft industry. For VAWTs, the working regimes are different, namely with higher α and lower Re . This makes the usual studied airfoils ill-fitted for VAWTs^[1-3]. It was demonstrated that for the NACA 4 digits airfoils, using airfoils with higher thickness (over 18%) increased performance^[1].

It was thought that the use of airfoils with camber would not be successful because as α changes sign each half turn, any gain obtained with α positive would be lost when α was negative. The Sandia laboratories and Kirke^[2] tested VAWTs equipped with cambered airfoils and concluded that the use of cambered airfoils had increased $C_{p_{max}}$ and $\lambda_{optimum}$ ^[1].

One greatest disadvantage of lift VAWTs is the usual lack of automatic start-up. Many solutions have been presented, most commonly the use of drag elements, obtaining a hybrid lift-drag VAWT. According to Kirke^[2], on the other hand, drag elements with an area lower than 10% of the VAWT's area

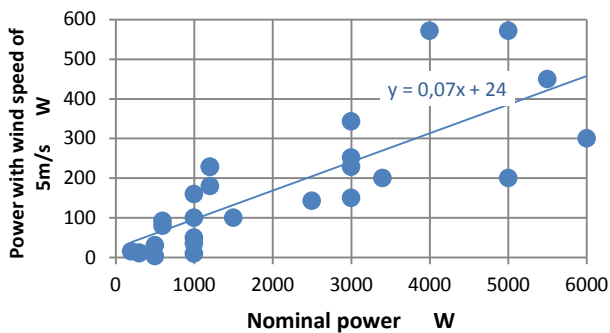
have little effect. He also says that the more viable current solutions are the use of cambered airfoils, flexible blades or passive pitch control techniques.

III. SIMILAR SYSTEMS

Data from small commercially available VAWTs was obtained based from reference [13]. This data was compiled in a database used to evaluate important parameters in the development of VAWTs.

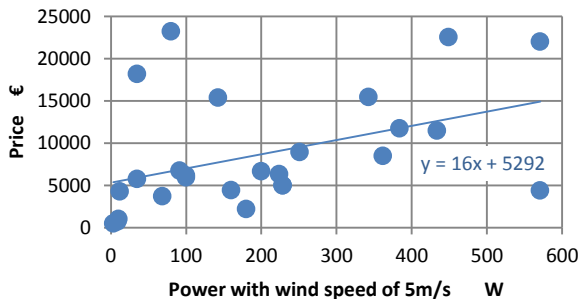
VAWTs usually indicate the nominal power, produced at $V_{rated} \cdot V_{rated}$ is usually high (10-16m/s) making the values presented inappropriate for most locations. The correct method for estimating energy production is by analyzing the probability distribution of wind speed and the power curve of the turbine.

To compare different parameters amongst VAWTs according to power developed, it is important to set a common condition for power production. This condition was set as $V_{\infty} = 5$ m/s. Nominal power was compared to power produced at $V_{\infty} = 5$ m/s (Graph 2).



Graph 2 – Power produced at $V_{\infty}=5$ m/s vs nominal power

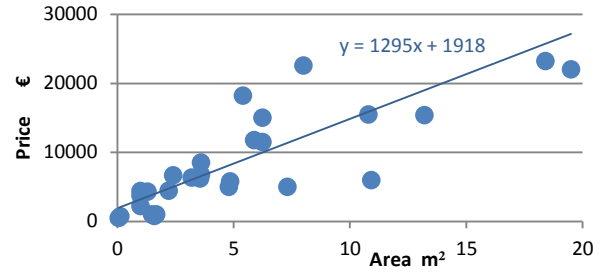
The cost of VAWTs was compared as shown in Graph 3.



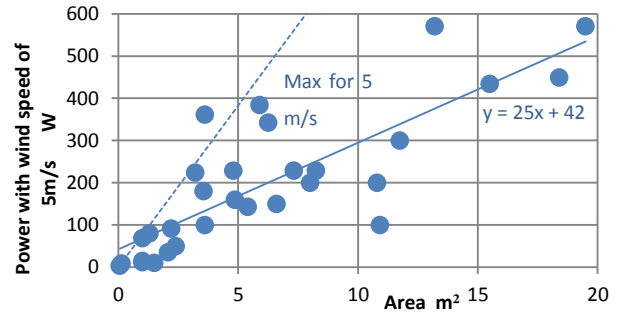
Graph 3 – Price according to power produced at $V_{\infty}=5$ m/s

The values obtained depend on many factors such as location, transport, taxes, warranties, etc. For the database, the values present the cost of the complete VAWT, in the place of production (no transport or assembly). There is a wide range of values, explained by the differences in the product's quality and the fact that this is a recent and growing market where competition needs to settle.

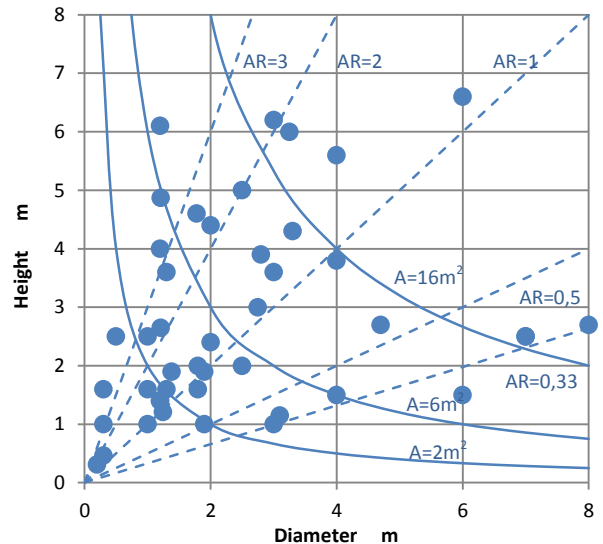
To analyze the A and AR of the VAWTs, Graph 4, Graph 5 and Graph 6 were obtained.



Graph 4 – Price vs area



Graph 5 – Power produced at $V_{\infty}=5$ m/s vs area



Graph 6 – AR analysis of VAWTs

The small range of areas compiled does not allow a complete analysis of the price evolution according to the area. Graph 6 presents the results of 42 VAWTs with full lines representing the area and dotted lines the AR . Though VAWTs with $AR > 1$ are 2/3 of the total, there are many VAWTs with low AR . This parameter is mainly associated with the type of generator used, as explained before. From the analyzed VAWTs, most use a direct drive, permanent magnet generator developed intentionally. The number of blades varies between 3 and 5, 5 being the most common value.

IV. AERODYNAMIC ANALYSIS

A. State of the art

Nowadays a complete theoretical procedure for the development of a VAWT does not exist. Most development

is done by obtaining results for many configurations by numerical computation^[1]. Many aerodynamic models have been developed for VAWTs such as the double/multiple streamtube model, the vortex model and the cascade model. These models usually contain various components, developed in the following order:

- Calculation of V_p , according to θ , λ , r and V_∞ ;
- Calculation of the aerodynamic forces applied in the blades;
- Calculation of the VAWT induced velocity (different from the airflow's speed due to the interaction of the turbine over the flow);
- Calculation of tridimensional effects;
- Consideration of dynamic stall^[1,8].

Computational fluid dynamics has been used with success for wind turbines. Although at the cost of great computational effort, CFD is able to simulate dynamic stall. The results obtained depend on the model used, the mesh parameters and the convergence criteria^[1]. 3D CFD of VAWTs requires, at least, 30 times more computational capacity than 2D simulations.^[14]

Wang^[15], used the kw SST model to study a giromill VAWT and concluded that this model provides results similar to experimental data. He also concluded that for the simulation of giromill VAWTs, the kw SST transitional model should be preferred to models ke, Spalart-Allmaras or Baldwin-Lomax. Howell^[10] indicates that the CFD ke standard model has low accuracy results.

B. Analysis made

Results were obtained using CFD. The kw SST transitional model was chosen given the good results previously obtained by investigators of IST and Wang^[15]. The results were obtained for a VAWT giromill similar to the prototype that would later be developed. The prototype is small to reduce costs, building time and to facilitate testing. The VAWT simulated has $r=0,5m$, the $c=5$ or $10cm$ long. The number of blades varies between 2 and 5. The airfoils used are the NACA0012 and NACA0018 due to the extensive information available and the recommendation from IST investigators. Using these parameters, 7 configurations were tested as shown in Table 1 .

Configuration	Airfoil	c mm	n	σ
1	NACA0018	50	3	0,3
2			2	0,2
3			4	0,4
4	NACA0018	100	2	0,4
5			3	0,6
6	NACA0012	50	5	0,5
7			3	0,3

Table 1 – Configurations analyzed with CFD

The configurations were chosen to allow the study of different parameters such as AR , σ or the airfoils used. Each configuration was simulated with several values of V_∞

and λ . For each simulation, M , F_x and F_y were obtained. The results were obtained using the *Fluent*[®] software. The meshes were obtained with the *Gambit*[®] software. Along the central post and the blades, a tight mesh was applied to correctly reproduce the conditions of the boundary layer (Figure 3).

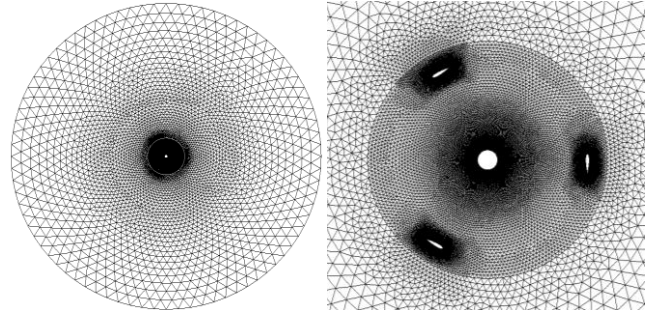


Figure 3 – Mesh used for CFD (left) and detail for configuration 5 (right)

All calculations were made using a laptop. The time spent for the calculation and the preparation of all conditions was over 6 months. For each test, the results were obtained in the 4th turn. This was necessary as in the first few turns the results had to stabilize. Some results are presented in Figure 4 and Figure 5.

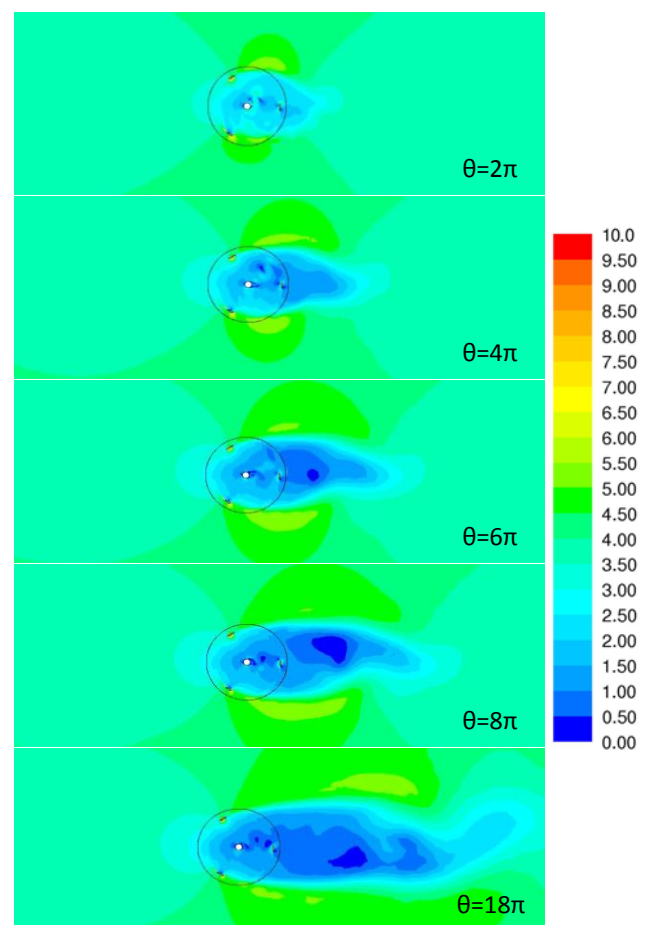


Figure 4 – $|V|$ for configuration 5 with $V_\infty=4m/s$, $\lambda=4$

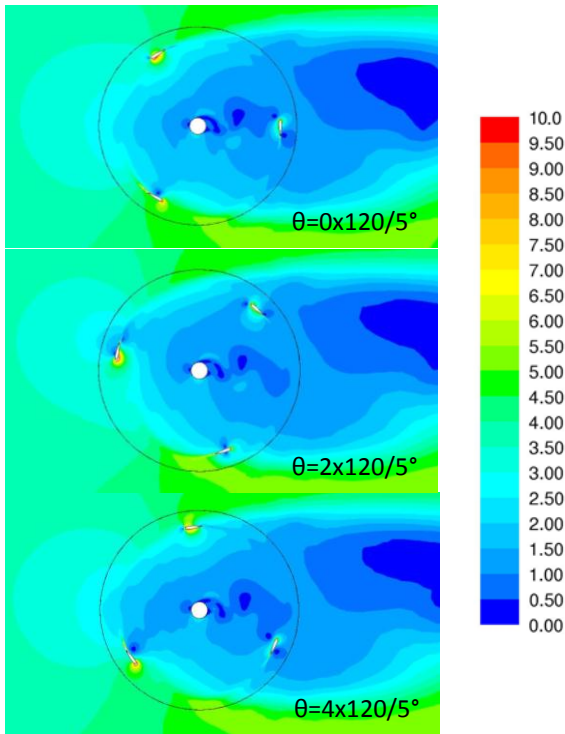
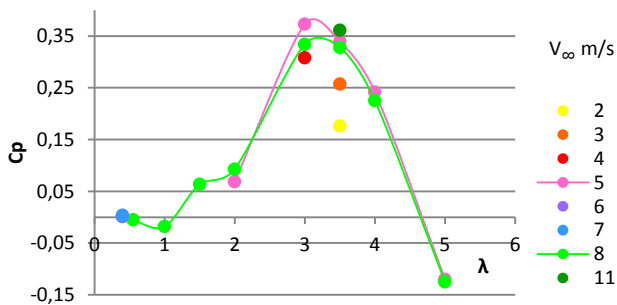


Figure 5 - $|V|$ for configuration 5 with $V_\infty=4\text{m/s}$, $\lambda=4$ (detail at 4th turn)

The results obtained suggest a correct simulation of the physical phenomena involved. There is an alternate vortex formation after the central pole. There's also, as expected, a deficit of V_∞ inside and after the turbine. This is important to understand the importance of the development of theoretical models with momentum balance.

Graph 7 shows an example of the results obtained for configuration 5, where spline curves for $V_\infty = 5\text{ m/s}$ and $V_\infty = 8\text{ m/s}$ were added to facilitate the visualization.

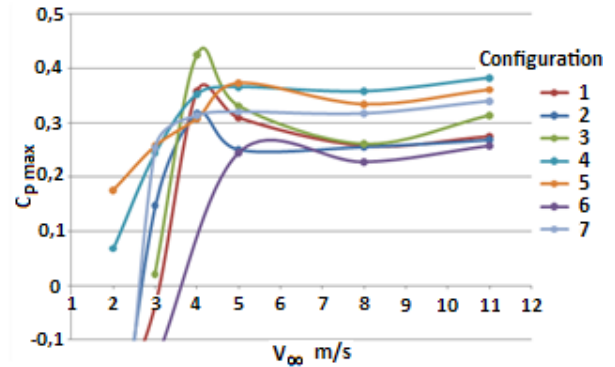


Graph 7 – CFD results for configuration 5

A compilation of the results obtained is shown in Graph 8. Not all values of V_∞ and λ were tested for each configuration, so the value of $C_{P_{\max}}$ presented refers to the maximum value obtained. As more conditions were obtained for $V_\infty = 5\text{ m/s}$ and $V_\infty = 8\text{ m/s}$, in this range of values the results presented are expected to have better accuracy.

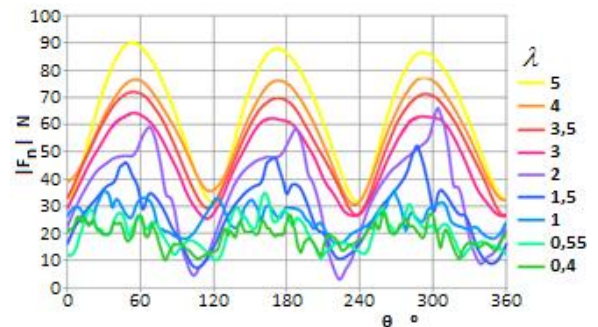
With these results, we start to evaluate all the configurations with NACA0018 airfoils (all configurations except number 7). The configurations with $c = 100\text{ mm}$ (4

and 5) yielded better results (about 40%) than the configurations with $c = 50\text{ mm}$ (1, 2, 3 and 6). Even for configurations with equal σ , such as configurations 3 and 4, configuration 4 with higher c has better results. Within the configurations with $c = 50\text{ mm}$ (1, 2, 3 and 6), the best result is obtained for $\sigma = 0,4$ (configuration 3), existing configurations with σ inferior and superior with worst results. To compare the effect of different airfoils, we can compare configuration 1 (NACA0018) and 7 (NACA0012). Configuration 7, equipped with NACA0012 airfoils yielded better results than configuration 1 (about 30%).



Graph 8 – $C_{P_{\max}}$ according to V_∞ for all configurations

Another important evaluation refers to the lateral forces. Graph 9 shows $|F_n|$, along θ for several values of λ .

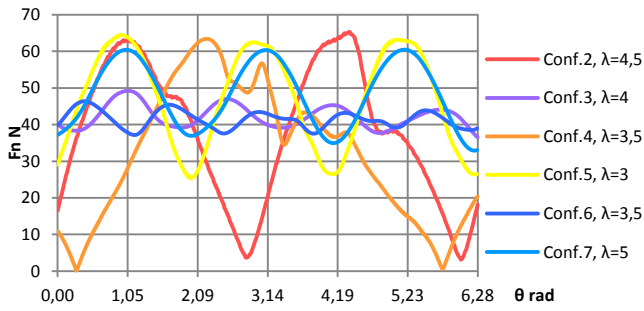


Graph 9 - $|F_n|$ according to θ for conf. 5 with $V_\infty=8\text{m/s}$

$|F_n|$ reaches a certain regularity for high values of λ . As the working regime is usually at high λ (higher C_P), the more irregular curves may be considered transitional regimes. The other curves, have a sinusoidal form with variable intensity but approximately constant f . For the same configuration, similar results are obtained for different values of V_∞ . Graph 10 depicts $|F_n|$ for the other configurations with $V_\infty = 8\text{ m/s}$ and λ_{optimum} .

The sinusoidal behavior is only presented for configurations with 3 (configurations 5 and 7) and 4 blades (configuration 3). The other configurations have a closely sinusoidal pattern but with distortions. In these cases, $|F_n|$ has more than one f , making more difficult the dynamic

behavior analysis of the turbine. Also, the intensity of $|F_n|$ varies with each configuration.



Graph 10 - $|F_n|$ according to θ for several configurations with $V_\infty=8$ m/s and λ_{optimum} .

V. BUILDING THE VAWT PROTOTYPE

To validate the numerical results previously obtained, a VAWT prototype was designed and built.

A. Bibliographic review

Parashivoiu^[1] refers that the most promising developments in VAWTs are the use of guy cables, truss columns and composite materials. Nowadays, turbine's blades are usually built with composites with carbon or glass fibers with polyester or epoxy. The interior is filled with sandwich structures composed of PVC, PET or even balsa wood^[16].

The end-of-life disposal of the turbine is also very important. The amount of materials used should be minimum and recyclable (in 2030, near 225000 tons of blades are expected to reach end-of-life). Nowadays only 30% of a fiber reinforced plastic composite can be recycled as new composite. The rest of it can be used as a filling material in construction but most of the blades are reduced in size (a difficult process) and combusted^[17].

For small VAWTs, the best option is the use of easily recyclable plastics (such as PET) and the development of a VAWT easily dismantable and with fewer different materials.

B. Building the prototype

It was expected to build a prototype able to change several parameters such as the number of blades or the blade's airfoil. To achieve this, a modular design, allowing the use of different modular pieces was developed. The prototype designed was also small and simple to reduce costs, ease testing and allow a fast construction.

The blades were built in the Aerospace department of IST using a hot-wire computer controlled machine. The machine was used to cut the airfoil shape from an insulating foam board. A layer of fiber glass was then applied to the foam blades.

The maximum length of the blades was limited by the hot-wire machine to approximately 1m. The blades were built

with this maximum dimension to increase the AR of the turbine, diminishing the influence of tridimensional effects.

The rest of the prototype was built in a specialized shop (Figure 6).



Figure 6 – Prototype built (without instruments)

It is composed of a central pole attached by two bearings to a wider central pole. Two disks are attached to the external central pole allowing the connection of different sets of arms that support the blades. It is possible to test configurations from 1 to 7 blades. Figure 7 and Figure 8 depict some details.

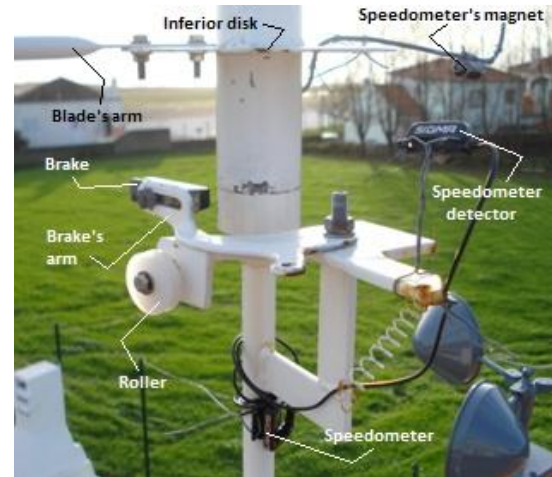


Figure 7 – Prototype detail

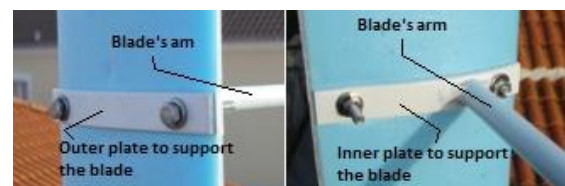


Figure 8 – Prototype detail

VI. TESTING THE PROTOTYPE

A. Bibliographic review

To test the efficiency of a VAWT, it is necessary to control λ applying a known M . It is also necessary to measure V_∞ and ω . The measure of P can be made directly using dedicated equipment or through M and ω .

In similar tests, several sensors were used such as pressure sensors, accelerometers or extensometers^[1,2,11]. The use of various sensors allows for a more detailed set of data, which is important for the complete study of the turbine

configuration^[19]. Other interesting tests were made using other techniques such as acoustic emissions or interferometric techniques^[21].

Sheldahl^[20] and Parashivoiu^[1] say that testing a turbine in real conditions is hard due to the variability of wind and the subjection to weather conditions. To avoid this, the use of high sample rate systems is recommended.

B. Tests made

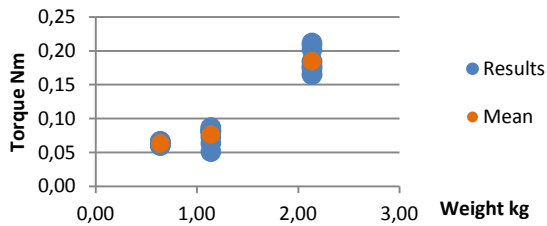
For testing the turbine, a cup anemometer, a speedometer, and a system of weights coupled to a brake, were used. The speedometer was used to obtain ω . A bicycle speedometer was used. The sensor was attached to the blades. The value measured was the linear velocity of the blade in km/h.

The brake was used to apply a known M to the turbine. To calibrate the brake, a series of tests were conducted. Also, it was necessary to calculate the turbine's M due to effects such as rolling friction. Both were calculated the same way.

First the turbine (without blades) was placed horizontally with a cable rolled in the outer central pole. In the end of the rolled cable, a known weight was tied. Next, the turbine was allowed to rotate freely. Given the effect of the weight, the turbine started to spin, unrolling the cable. The time taken for the weight to cover a certain distance is related to M in Nm according to

$$M = Pr - \frac{2II}{rt^2}. \quad (18)$$

The moment of inertia of the turbine was calculated as $I = 0,01089918 \text{ kgm}^2$. The results obtained are presented in Graph 11.



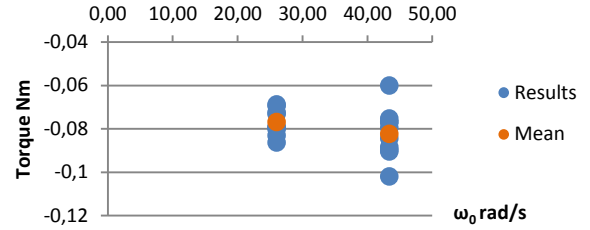
Graph 11 – Measurement 1 for the brake's calibration

The M obtained varies with the P used. This was explained by the existence of lateral forces in the bearings that increase the rolling friction. To avoid this, the turbine should be tested without exerting lateral forces on it. This was done by placing the VAWT vertically in its correct position. The VAWT was then accelerated using a drill until a known constant ω_0 was obtained. Then the drill was decoupled from the turbine allowing it to rotate freely.

The time t in s taken for the turbine to stop is related to M in Nm as

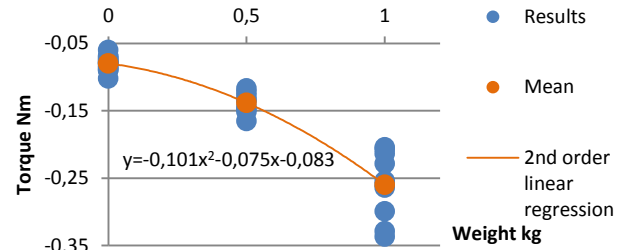
$$|M| = \frac{\omega_0 I}{t}, \quad (19)$$

The results obtained are presented in Graph 12.



Graph 12 – Measurement 2 for the brake's calibration

M obtained is approximately constant. From these results it can be concluded that there is not an important variation of M with ω . Using the same test conditions, the brake was calibrated obtaining the results presented in Graph 13.



Graph 13 – Measurement 3 for the brake's calibration

It is important to notice that even at high ω_0 , no disequilibrium or vibrations were noticed in the turbine's movement. Under these conditions it was assumed that the main inertial axis was correctly aligned with the turbine's rotation axis.

It was hard to conciliate the tests with the weather conditions given the season (the tests began in December) and the highly variable weather conditions in the Azores. The prototype should be tested during daylight, without rain with near constant wind. Such conditions rarely occurred.

To test the prototype, a known M was applied to the turbine using the break. Then when V_∞ and ω stood approximately constant for at least 20s, the values were registered.

To start-up the turbine, it is usually necessary to reach a minimum ω . Figure 9 depicts this situation.

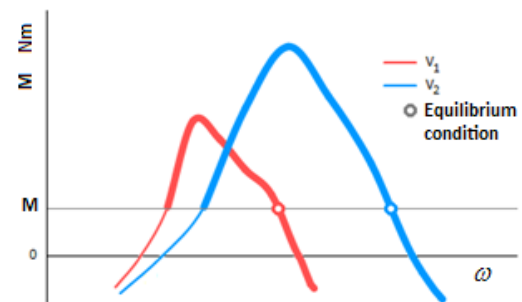


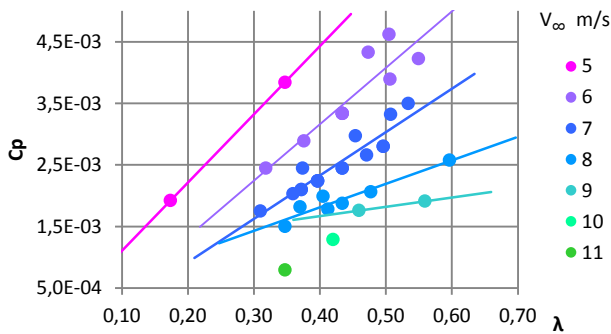
Figure 9 – VAWTs working principle

Consider a turbine that respects the curves presented for two wind speeds, V_1 and V_2 . Consider M_0 the torque applied in the turbine (considered constant). Consider that

the wind speed remains V_1 . Consider that the turbine is under the working conditions of the thin line of the graph, producing a torque lower than M_0 . Under these circumstances, the angular acceleration is negative, diminishing ω until the turbine stops. Now consider that the turbine is under the working conditions of the bold line of the graph, producing a torque higher than M_0 . Under these conditions, the turbine accelerates until it reaches the equilibrium condition presented in the graph. In the same previous conditions (bold line), if the torque produced by the turbine is lower than M_0 , ω will diminish until the equilibrium condition is reached.

To experimentally obtain the curve of the turbine, without the possibility to measure the angular acceleration, it is necessary to vary M_0 . The stabilization of the turbine in a given ω with constant V_∞ , means that the equilibrium condition has been reached and the values can be registered.

Configuration 5 was the first to be tested because it was expected to have better stability (3 blades) and higher structural resistance (blades with 10cm chord). It was expected, given the numerical results, that it would be necessary to accelerate the turbine to start-up. But it was discovered that the turbine started to rotate without any help, although only reaching small values of λ (under 0,6). Numerical calculations for low λ were obtained. It was discovered that the configuration had another working area at low λ . As it was intended to test the turbine under the conditions previously calculated (high λ values), the turbine was accelerated using a drill. But this led to extreme vibrations in the turbine's structure that made the tests under these conditions unreachable. Results were obtained for low λ as shown in Graph 14.



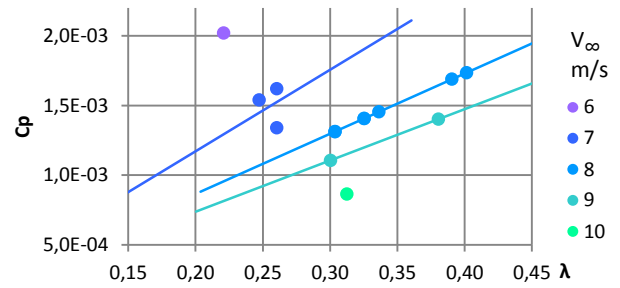
Graph 14 – Field results for configuration 5

The brake was not applied so $M = 0,083$ Nm. Linear regressions are presented for each V_∞ . The higher the V_∞ , the smaller the linear regression decay. This was expected as

$$C_p = \frac{M\omega}{\frac{1}{2}\rho AV_\infty^3} \Leftrightarrow C_p \propto \frac{\lambda}{V_\infty^2}. \quad (20)$$

For $V_\infty = 8$ m/s and $M = 0,083$ Nm there is an equilibrium condition at $\bar{\lambda}_{field} = 0,440 \pm 0,073$. The numerical calculations present an equilibrium condition at $\lambda_{CFD} = 0,386$. It should also be noticed that this condition is found for $M = 0,083$ Nm however, as presented before, there are lateral forces applied in the bearings that affect M . According to Graph 9, $10 < F_n < 35$ N which according to Graph 11 $M > 0,2$ Nm. During the tests, the measurement of F_n could have been made with extensometers or accelerometers. Without a real measure of F_n , the analysis of results is made for $M = 0,083$ Nm.

Results were also obtained for configuration 4: NACA0018, 2 blades with $c=10$ cm. Results similar to configuration 5 were obtained, which also led to the calculation of numerical results at low λ .



Graph 15 – Field results for configuration 4

An equilibrium condition was found for $\lambda_{field} = 0,346 \pm 0,043$ at $V_\infty = 8$ m/s. The numerical calculations present an equilibrium condition for $\lambda_{CFD} = 0,300$.

To validate the results obtained it's important to evaluate the errors during the experiments. The turbine tested is a tridimensional system, subjected to effects that are not accounted during bidimensional numerical calculations. The blades have tolerances, roughness, are not rigid and are not perfectly tangential to the trajectory. The turbine itself is not rigid, affecting the flow conditions. The central pole has less 5cm in the prototype than in the numerical calculations. It also has bonded structures, such as the supporting discs, that affect the flow. The flow conditions in the field are not ideal. The wind has turbulence and varies its direction and intensity. It also has variable properties such as temperature and density.

The anemometer used is the only calibrated equipment, with a resolution of 10m. It has high inertia, working as a low pass filter in the measurement of wind speed intensity. The speedometer has a resolution of 0,1km/h and the chronometer a resolution of 0,1s. Several trials were made for each test condition to determine the measurement precision and accuracy. In the graphs presented, many of the results obtained are overlaid due to the instrument's resolution.

With all these limitations, the results achieved, with overlap or close overlap of numerical and field results are very encouraging (Table 2).

Test	Equilibrium condition for $V_{\infty}=8\text{m/s}$, $M=0,083\text{Nm}$	
	λ_{CFD}	λ_{field}
Configuration 4	0,300	0,346±0,043
Configuration 5	0,386	0,440±0,073

Table 2 – Analysis of the results obtained

However, it is important to notice that results were only obtained for two configurations, in a very restrictive range of V_{∞} and λ .

VII. CONCLUSIONS

The work enabled an important analysis of the fundamentals of VAWTs. Several conclusions were achieved:

- VAWTs are complex systems, with difficult analysis, little information available and insufficient dedicated research.
- The numerical simulation of VAWTs using the kw SST model offers the expected description of physical phenomena with results similar to those obtained experimentally. However, the restrict range of experimental results did not allow for a complete analysis of the model. Regardless, the numerical results obtained are an important source of data for work in this area.
- From the configurations numerically calculated, configuration 4 (2 NACA0018 blades with $c=10\text{cm}$ and $r=0,5\text{m}$) is the one that presented the best results. Nevertheless, very few configurations were tested for a final conclusion and the choice of an optimum configuration also depends on other factors that were not fully evaluated.
- The test of VAWTs in real conditions is difficult. Further attempts should be made using equipment with high sample rates and automatic data collecting. The turbine itself should be resilient and able to stand outside for long periods of time.
- The high differences obtained in C_p with each configuration show that small changes in the parameters of a VAWT greatly affect its performance. This seems promising as there may be configurations with characteristics that will provide VAWTs as a reliable and highly valuable type of wind turbine.

REFERENCES

1. **Paraschivou, Ion.** *Wind turbine design (with emphasis on Darrieus concept)*. École Polytechnique de Montréal. ISBN 2-553-00931-3, 2002.
2. **Kirke, Brian Kinloch.** *Evaluation of self-starting vertical axis wind turbines for stand-alone applications*. Phd thesys, Griffith University, 1998.
3. **Manwell, J. F., McGowan, J. G. and Rogers, A. L.** *Wind energy explained (theory, design and application)*. John Wiley & Sons Ltd. ISBN 0-470-84612-7, 2002.
4. **EWEA.** *Wind energy: the facts*. EWEA. 2009.
5. **EWEA.** *Oceans of opportunity – Harnessing Europe’s largest domestic energy resource*. EWEA. 2009.
6. **EWEA.** *The economics of wind energy*. EWEA. 2009.
7. **White, Frank M.** *Fluid mechanics*. McGraw-Hill. ISBN 978-0-07-128645-9. 6th edition.
8. **Islam, Mazharul, Ting, David and Fartaj, Amir.** *Aerodynamic models for Darrieus-type straight-bladed vertical axis wind turbines*. Renewable & sustainable energy reviews. 2008, Vols.12 pp.1419-1434.
9. **Fujisawa, Nobuyuki and Shibuya, Satoshi.** Observations of dynamic stall on Darrieus wind turbine blades. Journal of wind engineering and industrial aerodynamics. 2001, Vols.89 pp.201-214.
10. **Howell, Robert et al.** *Wind tunnel and numerical study of a small vertical axis wind turbine*. Renewable energy. 2010, Vols.35 pp.412-422.
11. **Ashwill, Thomas.** *Measured data for the Sandia 34-meter vertical axis wind turbine*. Sandia laboratories report SAND91-2228. 1992.
12. **van Bussel, Gerard.** *The development of Turby, a small VAWT for the built environment*. Global wind energy conference. 2004.
13. **All Small Wind Turbines.** <http://www.allsmallwindturbines.com/>. 2010.
14. **Li, Ye and Calisal, Sander.** *Three-dimensional effects and arm effects on modeling a vertical axis tidal current turbine*. Renewable energy. 2010, Vols.35 pp.2325-2334.
15. **Wang, Shengyi et al.** *Numerical investigations on dynamic stall of low Reynolds number flow around oscillating airfoils*. Computers & fluids. 2010, Vols.39 pp.1529-1541.
16. **Reuterlov, Stefan.** *The role of sandwich composites in turbine blades*. Reinforced plastics. 2002, Vols. March 2002 pp.32-34.
17. **Larsen, Kari.** *Recycling wind turbine blades*. Renewable energy focus. 2009, Vols. Jan/Feb 2009 pp.70-73.
18. **Habali, S. and Saleh, I.** Local design, test and manufacturing of small mixed airfoil wind turbine blades of glass reinforced plastics. Part II: Manufacturing of the blade and rotor. *Energy conversion & management*. 2000, Vols. 41 pp.281-298.
19. **Zayas, Jose, Jones, Perry and Holman, Adam.** *CX-100 and TX-100 blade field tests*. Sandia laboratories report SAND2005-7454. 2005.
20. **Sheldahl, Robert.** *Comparison of field and wind tunnel Darrieus wind turbine data*. Sandia Laboratories report SAND802469-2228. 1981.
21. **Rumsey, Mark et al.** *Experimental results of structural health monitoring of wind turbine blades*. Sandia laboratories. 2007.